Pergamon

Int. J. Solids Structures Vol. 31, No. 11, pp. 1519–1536, 1994

0020–7683/94 $7.00 + .00

0020–7683(93)E0041–F

VIBRATION OF PERFORATED DOUBLY-CURVED SHALLOW SHELLS WITH ROUNDED CORNERS

K. M. LIEW and C. W. LIM
Dynamics and Vibration Centre, School of Mechanical and Production Engineering,
Nanyang Technological University, Nanyang Avenue, Singapore 2263

(*Received* 31 *March* 1993; *in revised form* 1 *December* 1993)

Abstract—This study examines the natural frequency and vibratory characteristics of doubly-curved shallow shells having an outer super-elliptical periphery and an inner super-elliptical cutout. A super-elliptical boundary in this context is defined as $(2x/a)^{2n}+(2y/b)^{2n} = 1$, where $n = 1, 2, 3, \ldots, \infty$. This class of shells with rounded outer and inner corners has a great advantage over shells with a rectangular planform as stress concentration at the corners is greatly diffused. As a result, the high stress durability of such shells has a great potential for use in practical engineering applications, especially in aerospace, mechanical and marine structures. The doubly-curved shells investigated possess variable positive (spherical), zero (cylindrical) and negative (hyperbolic paraboloidal) Gaussian curvatures. A global energy approach is proposed to the study of such shell problems. The Ritz minimization procedure with a set of orthogonally generated two-dimensional polynomial functions is employed in the current formulation. This method is shown to yield better versatility, efficiency and less computational execution than the discretization methods.

1. INTRODUCTION

The vibration of shallow shells (Leissa, 1973a) has long been a subject of intensive research for many years. A vast number of references can be found for such analyses of cylindrical and spherical shallow shells (Webster, 1968; Deb Nath, 1969; Petyt, 1971; Olson and Lindberg, 1971; Leissa *et al.*, 1983; Leissa and Narita, 1984; Cheung *et al.*, 1989). However, the literature dealing with shells with circular and elliptical planforms is limited. To the authors' knowledge, the only study was done by Narita and Leissa (1986) who investigated the completely free shallow shells of curvilinear planform.

Rectangular plates with rounded corners, the so-called super-elliptical plates, had been examined by Irie *et al.* (1983) and Wang *et al.* (1993). The doubly-connected plates of arbitrary shape with over-restrained boundaries have been treated recently by Liew (1993). No studies can be found for flexural vibration of doubly-curved shallow shells with an internal cutout having super-elliptical inner and outer peripheries. This class of shells, however, has many possible engineering applications, especially in aerospace, mechanical and marine structures, owing to its capability to diffuse and dilute stress concentration at the rounded corners and thus possesses higher stress durability. It is, therefore, the primary motivation of the current paper to investigate the vibration behaviour of this class of perforated shallow shells. With the aim of enhancing the literature, a set of comprehensive natural frequencies and mode shapes of such shells subject to various boundary constraints is presented.

The eigenvalue derivation, in this paper, is based on the Ritz minimization procedure. A class of admissible *pb*-2 shape functions is employed (Lim and Liew, 1994; Liew and Lim, 1994a, b). These *pb*-2 shape functions consist of the product of sets of orthogonally generated two-dimensional polynomial functions (*p*-2) and a basic function (*b*). These kinematically oriented shape functions ensure automatic satisfaction of the prescribed geometric boundary conditions at the outset. As a result, this method of analysis prevails over the discretization methods in terms of versatility, efficiency and computation effort with no loss of (or even better) accuracy.

The present undertaking covers wide ranges of curvature ratios and shallowness ratios with selective super-elliptical shell geometries. Results of rectangular shells with a circular cutout is also presented to emphasize the consistency and accuracy of frequencies between the super-elliptical and rectangular shells. The convergence and comparison tests of eigenvalues are examined to ensure the numerical accuracy and reliability of these results. Sets of non-dimensional frequency parameters and mode shape figures are presented for future reference.

2. THEORETICAL FORMULATION

2.1. *Problem definition*

Consider a homogeneous, isotropic and thin perforated doubly-curved shallow shell bounded by a super-elliptical boundary with thickness h and radii of curvature R_x and R_y. The geometric expression of the midsurface of the shell in rectangular cooordinate system is given as

$$z = -\frac{1}{2}\left(\frac{x^2}{R_x}+\frac{y^2}{R_y}\right) \tag{1}$$

and the super-elliptical circumferences can be represented by

$$\left(\frac{2x}{a}\right)^{2n}+\left(\frac{2y}{b}\right)^{2n} = 1; \quad n = 1,2,3,\ldots,\infty, \tag{2}$$

where a and b are the maximum shell dimensions in the x- and y-directions, respectively. The shell is doubly-connected with a super-elliptical cutout of dimensions a' and b'. Figure 1 shows the planform of the shell where $2n_1$ and $2n_2$ are the powers of the super-elliptical functions of the outer and inner peripheries. The deflections of the midsurface are resolved into three orthogonal components u, v and w, with u and v tangential to the midsurface (u parallel to the xz-plane and v parallel to the yz-plane) and w normal to it.

The free vibration frequencies and mode shapes of this perforated super-elliptical shell are determined using the Ritz formulation. Two classes of perforated shells are under the present consideration: (1) simply supported and (2) fully clamped shells on the outer circumferences. Both shells have the inner boundaries free. These boundary constraints are termed SF and CF (where S and C stand for the simply supported and fully clamped outer circumferences, respectively, and F the free inner boundary).

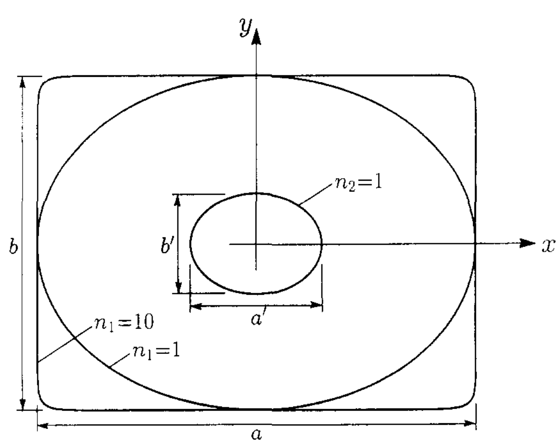

Fig. 1. Geometry of the planform of super-elliptical shell $(2x/a)^{2n_1}+(2y/b)^{2n_1} = 1$ with a super-elliptical cutout $(2x/a')^{2n_2}+(2y/b')^{2n_2} = 1$.

2.2. *Energy functional*

The total strain energy, $\mathscr{U}$, of the shell described above is composed of the membrane strain energy, $\mathscr{U}_s$, and the bending strain energy, $\mathscr{U}_b$

$$\mathscr{U} = \mathscr{U}_s + \mathscr{U}_b. \tag{3}$$

The membrane strain energy is caused by the stretching effects of the midsurface of the shell. The strain energy components are respectively given by (Leissa *et al.*, 1983)

$$\mathscr{U}_s = \frac{6D}{h^2}\int\int_A \left[(\varepsilon_x+\varepsilon_y)^2 - 2(1-\nu)\left(\varepsilon_x\varepsilon_y - \frac{1}{4}\gamma_{xy}^2\right)\right] \mathrm{d}A \tag{4}$$

and

$$\mathscr{U}_b = \frac{D}{2}\int\int_A \left\{(\Delta w)^2 - 2(1-\nu)\left[\frac{\partial^2 w}{\partial x^2}\frac{\partial^2 w}{\partial y^2} - \left(\frac{\partial^2 w}{\partial x\,\partial y}\right)^2\right]\right\} \mathrm{d}A, \tag{5}$$

where the flexural rigidity $D = Eh^3/12(1-\nu^2)$, E is Young's modulus, ν is the Poisson ratio, A is the shell planform area and Δ is the Laplacian operator defined as $(\partial^2/\partial x^2 + \partial^2/\partial y^2)$. The double integration is performed over the projected planform area of the shell on the xy-plane.

The strains of the membrane can be expressed in terms of the deflections as

$$\varepsilon_x = \frac{\partial u}{\partial x} + \frac{w}{R_x}; \quad \varepsilon_y = \frac{\partial v}{\partial y} + \frac{w}{R_y}; \quad \gamma_{xy} = \frac{\partial v}{\partial x} + \frac{\partial u}{\partial y}. \tag{6a–6c}$$

The kinetic energy is given by

$$\mathscr{T} = \frac{\rho h}{2}\int\int_A \left[\left(\frac{\partial u}{\partial t}\right)^2 + \left(\frac{\partial v}{\partial t}\right)^2 + \left(\frac{\partial w}{\partial t}\right)^2\right] \mathrm{d}A, \tag{7}$$

where ρ is the mass density per unit volume.

Assuming the free vibration amplitude to be small, the deflection functions may be expressed as sinusoidal functions

$$u(x, y, t) = U(x, y)\sin\omega t \tag{8a}$$

$$v(x, y, t) = V(x, y)\sin\omega t \tag{8b}$$

$$w(x, y, t) = W(x, y)\sin\omega t, \tag{8c}$$

where ω is the angular frequency of vibration. By using eqns (6a–c) and (8a–c), the strain energy and kinetic energy components, eqns (4), (5) and (7), can be further simplified to the following expressions

$$\begin{aligned}(\mathscr{U}_s)_{\max} = \frac{6D}{h^2}\int\int_A \Bigg\{&\left(\frac{\partial U}{\partial x}\right)^2 + 2\frac{W}{R_x}\frac{\partial U}{\partial x} + \left(\frac{W}{R_x}\right)^2 + \left(\frac{\partial V}{\partial y}\right)^2 + 2\frac{W}{R_y}\frac{\partial V}{\partial y} + \left(\frac{W}{R_y}\right)^2 \\ &+ 2\nu\left(\frac{\partial U}{\partial x}\frac{\partial V}{\partial y} + \frac{\partial U}{\partial x}\frac{W}{R_y} + \frac{W}{R_x}\frac{\partial V}{\partial y} + \frac{W}{R_x}\frac{W}{R_y}\right) \\ &+ \frac{1-\nu}{2}\left[\left(\frac{\partial V}{\partial x}\right)^2 + 2\frac{\partial V}{\partial x}\frac{\partial U}{\partial y} + \left(\frac{\partial U}{\partial y}\right)^2\right]\Bigg\} \mathrm{d}A\end{aligned} \tag{9a}$$

$$(\mathscr{U}_b)_{\max} = \frac{D}{2}\int\int_A \left\{(\Delta W)^2 - 2(1-\nu)\left[\frac{\partial^2 W}{\partial x^2}\frac{\partial^2 W}{\partial y^2} - \left(\frac{\partial^2 W}{\partial x\,\partial y}\right)^2\right]\right\} \mathrm{d}A \tag{9b}$$

$$\mathscr{T}_{\max} = \frac{\rho h \omega^2}{2} \iint_A (U^2 + V^2 + W^2)\,\mathrm{d}A, \tag{9c}$$

where $(\mathscr{U}_b)_{\max}$, $(\mathscr{U}_s)_{\max}$ and $\mathscr{T}_{\max}$ denote the maximum bending strain, stretching strain and kinetic energies in a vibratory cycle. $U(x, y)$, $V(x, y)$ and $W(x, y)$ are the deflection amplitude functions in the x-, y- and z-directions.

2.3. *Eigenvalue equation*

In non-dimensional coordinates, $\xi = x/a$ and $\eta = y/b$, where a and b are the characteristic length scales of the shell planform as shown in Fig. 1. The deflection amplitude functions can be approximated by sets of orthogonally generated two-dimensional polynomials of the forms

$$U(\xi, \eta) = \sum_{i=1}^{m} C_i^u \phi_i^u(\xi, \eta) \tag{10a}$$

$$V(\xi, \eta) = \sum_{i=1}^{m} C_i^v \phi_i^v(\xi, \eta) \tag{10b}$$

$$W(\xi, \eta) = \sum_{i=1}^{m} C_i^w \phi_i^w(\xi, \eta), \tag{10c}$$

where C_i^u, C_i^v and C_i^w are the unknown coefficients. The *pb*-2 shape functions ϕ_i^u, ϕ_i^v and ϕ_i^w and the corresponding boundary conditions will be discussed in due course.

Minimization of the energy functional with respect to the unknown coefficients according to the Ritz principle as follows:

$$\frac{\partial}{\partial C_i^\alpha}(\mathscr{U}_{\max} - \mathscr{T}_{\max}) = 0, \quad \alpha = u, v \text{ and } w \tag{11}$$

in which $\mathscr{U}_{\max} = (\mathscr{U}_s)_{\max} + (\mathscr{U}_b)_{\max}$, results in the following governing eigenvalue equation

$$(12\mathbf{K} - \lambda^2 \mathbf{M})\{\mathbf{C}\} = \{\mathbf{0}\}, \tag{12}$$

where $\mathbf{K}$ is the stiffness matrix and $\mathbf{M}$ is the mass matrix. The detailed expressions for eqn (11) and the elements of $\mathbf{K}$ and $\mathbf{M}$ are given in Appendices A and B, respectively. The eigenvalue, λ, in eqn (12) is the non-dimensional frequency parameter of the vibrating shallow shell to be studied in the present analysis.

2.4. *The* pb-2 *shape functions and boundary constraints*

The *pb*-2 shape functions for U, V and W are ϕ_i^u, ϕ_i^v and ϕ_i^w, respectively. These shape functions are fundamentally sets of admissible functions which are composed of the product of terms (indicated by i) of a two-dimensional orthogonally generated polynomial (p-2) and a basic function (b), i.e.

$$\phi_i^\alpha(\xi, \eta) = f_i(\xi\, \eta)\phi_1^\alpha - \sum_{j=1}^{i-1} \Xi_{ij}^\alpha \phi_j^\alpha, \tag{13}$$

where

$$\Xi_{ij}^\alpha = \frac{{}_1\Delta_{ij}^\alpha}{{}_2\Delta_j^\alpha} \tag{14a}$$

$${}_1\Delta_{ij}^\alpha = \iint_A f_i(\xi, \eta)\phi_1^\alpha \phi_j^\alpha \,\mathrm{d}\xi\,\mathrm{d}\eta \tag{14b}$$

$${}_2\Delta_j^\alpha = \iint_A (\phi_j^\alpha)^2 \,\mathrm{d}\xi\,\mathrm{d}\eta, \quad \alpha = u, v \text{ and } w. \tag{14c}$$

$\Sigma_{i=1}^{m} f_i(\xi, \eta)$ forms a set of p-2 functions. The basic function, ϕ_1^{α} is defined as the product of the equations of the continuous piecewise boundary geometric expressions each of which is raised to a basic power depending on the types of boundary constraints imposed on the shell, i.e.

$$\phi_1^{\alpha}(\xi, \eta) = \prod_{i=1}^{n_e} [\Gamma_i(\xi, \eta)]^{\gamma_i^{\alpha}}, \quad \alpha = u, v \text{ and } w, \tag{15}$$

where n_e is the number of supporting edges; Γ_i is the boundary expression of the ith supporting edge; and γ_i^{α} ($\alpha = u$, v and w) are the basic powers.

The Ritz method requires an admissible function which satisfies the geometric boundary conditions. The imposition of the powers to the basic functions, $\phi_1^{\alpha}(\xi, \eta)$, results in a class of kinematically oriented pb-2 shape functions consistent with the following geometric

Table 1(a). Convergence of $\lambda = \omega ab\sqrt{(\rho h/D)}$ for the doubly-connected super-elliptical and rectangular simply supported shallow shells with a circular cutout ($\nu = 0.3$, $a/b = 1.0$, $a'/b' = 1.0$, $a'/a = 0.3$, $a/h = 100.0$ and $n_2 = 1$)

	p			Mode sequence number							
n_1	u	v	w	1	2	3	4	5	6	7	8
	10	10	10	156.14	156.14	192.73	192.73	216.90	221.97	221.97	258.96
	10	10	12	155.75	155.76	192.44	192.44	216.55	221.31	221.31	258.92
	10	10	14	155.39	155.39	192.02	192.02	216.32	221.04	221.04	258.88
	10	10	16	154.90	154.90	191.61	191.61	216.26	220.87	220.87	258.64
	10	10	18	154.35	154.36	191.31	191.31	216.24	220.70	220.71	256.78
	10	12	18	152.57	153.16	191.00	191.06	212.78	219.05	219.18	256.31
	10	14	18	151.82	152.56	190.75	190.81	211.22	217.96	218.08	255.96
1	10	16	18	151.50	152.28	190.58	190.64	210.58	217.36	217.43	255.75
	10	18	18	151.34	152.16	190.49	190.52	210.31	217.07	217.11	255.63
	10	20	18	151.27	152.11	190.44	190.46	210.18	216.93	216.95	255.57
	12	20	18	149.99	150.41	190.24	190.25	207.70	214.76	214.78	255.10
	14	20	18	149.51	149.67	190.06	190.07	206.56	213.40	213.42	254.74
	16	20	18	149.31	149.35	189.93	189.93	206.09	212.74	212.75	254.50
	18	20	18	149.18	149.18	189.85	189.85	205.90	212.46	212.46	254.36
	20	20	18	149.08	149.08	189.81	189.81	205.83	212.29	212.29	254.29
	10	10	10	164.31	166.70	191.29	191.29	218.91	220.96	220.97	245.07
	10	10	12	164.02	166.44	191.18	191.18	216.95	216.95	218.67	243.42
	10	10	14	163.91	166.40	191.07	191.07	216.72	216.72	218.19	242.72
	10	10	16	163.79	166.33	190.89	190.89	216.65	216.65	217.99	241.86
	10	10	18	163.64	166.24	190.65	190.65	216.58	216.58	217.90	240.75
	10	12	18	160.84	161.61	190.30	190.60	213.23	215.36	215.43	240.52
	10	14	18	158.59	159.11	189.92	190.50	210.20	214.46	214.53	240.14
10	10	16	18	156.90	157.70	189.57	190.35	208.27	213.71	213.76	239.65
	10	18	18	155.82	156.97	189.29	190.15	207.07	213.03	213.30	239.09
	10	20	18	155.21	156.63	189.10	189.96	206.37	212.51	213.02	238.61
	12	20	18	151.67	152.26	189.07	189.75	202.31	210.71	211.38	238.45
	14	20	18	148.85	149.91	189.03	189.49	199.54	209.10	209.84	238.31
	16	20	18	146.91	148.76	188.97	189.22	197.81	207.82	208.39	238.17
	18	20	18	145.79	148.25	188.89	188.98	196.82	206.93	207.18	238.06
	20	20	18	145.28	148.01	188.80	188.80	196.27	206.34	206.34	237.95
	10	10	10	154.66	156.12	190.57	190.57	208.42	213.92	213.92	242.44
	10	10	12	154.43	155.91	190.45	190.45	208.09	213.51	213.51	241.79
	10	10	14	154.24	155.79	190.23	190.23	207.77	213.37	213.37	240.82
	10	10	16	153.99	155.63	189.96	189.96	207.64	213.29	213.29	239.60
	10	10	18	153.70	155.43	189.68	189.68	207.59	213.20	213.20	238.40
	10	12	18	151.88	153.04	189.29	189.60	204.71	212.05	212.12	238.03
	10	14	18	150.84	151.65	188.95	189.51	202.66	211.16	211.24	237.63
∞	10	16	18	150.09	150.96	188.68	189.38	201.58	210.32	210.69	237.21
	10	18	18	149.73	150.53	188.50	189.24	200.92	209.72	210.37	236.80
	10	20	18	149.52	150.32	188.39	189.12	200.58	209.30	210.19	236.49
	12	20	18	147.12	148.42	188.34	188.86	198.11	207.61	208.61	236.36
	14	20	18	145.55	147.55	188.29	188.58	196.64	206.34	207.18	236.23
	16	20	18	144.67	147.12	188.23	188.36	195.81	205.52	206.01	236.12
	18	20	18	144.23	146.90	188.16	188.20	195.38	205.05	205.21	236.03
	20	20	18	144.05	146.73	188.10	188.10	195.14	204.74	204.74	235.96

Table 1(b). Convergence of $\lambda = \omega ab\sqrt{(\rho h/D)}$ for the doubly-connected super-elliptical and rectangular fully clamped shallow shells with a circular cutout ($\nu = 0.3$, $a/b = 1.0$, $a'/b' = 1.0$, $a'/a = 0.3$, $a/h = 100.0$ and $n_2 = 1$)

	p			Mode sequence number							
n_1	u	v	w	1	2	3	4	5	6	7	8
	10	10	10	173.99	174.00	197.95	197.95	222.46	245.92	245.93	289.36
	10	10	12	173.46	173.46	197.15	197.15	222.28	245.52	245.52	289.22
	10	10	14	172.75	172.75	196.39	196.39	222.23	245.24	245.24	289.15
	10	10	16	171.95	171.95	195.86	195.86	222.22	244.95	244.95	289.12
	10	10	18	171.21	171.22	195.56	195.56	222.21	244.66	244.66	289.11
	10	12	18	169.46	170.02	195.13	195.21	218.80	242.84	242.98	288.36
	10	14	18	168.73	169.43	194.79	194.88	217.26	241.65	241.78	288.08
1	10	16	18	168.43	169.17	194.58	194.65	216.63	240.99	241.07	287.96
	10	18	18	168.30	169.05	194.46	194.51	216.37	240.66	240.70	287.92
	10	20	18	168.24	169.01	194.40	194.43	216.25	240.51	240.53	287.90
	12	20	18	166.99	167.40	194.09	194.11	213.71	238.15	238.17	287.47
	14	20	18	166.52	166.69	193.82	193.83	212.55	236.67	236.69	287.29
	16	20	18	166.35	166.40	193.63	193.64	212.07	235.94	235.95	287.22
	18	20	18	166.25	166.26	193.53	193.53	211.88	235.61	235.62	287.20
	20	20	18	166.17	166.18	193.48	193.48	211.81	235.44	235.44	287.19
	10	10	10	173.67	181.09	195.10	195.10	231.81	243.17	243.22	262.17
	10	10	12	173.45	180.78	194.98	194.98	231.57	234.12	234.12	261.13
	10	10	14	173.38	180.59	194.77	194.77	231.10	233.60	233.60	261.04
	10	10	16	173.27	180.38	194.45	194.45	230.92	233.45	233.45	261.01
	10	10	18	173.16	180.12	194.06	194.06	230.85	233.26	233.26	260.97
	10	12	18	168.32	177.15	193.78	193.92	224.91	231.36	231.68	260.24
	10	14	18	165.90	174.83	193.46	193.70	221.17	230.13	230.85	259.95
10	10	16	18	164.53	173.04	193.17	193.39	218.92	229.18	230.17	259.86
	10	18	18	163.82	171.89	192.93	193.02	217.57	228.53	229.66	259.80
	10	20	18	163.48	171.22	192.68	192.77	216.81	228.13	229.30	259.76
	12	20	18	159.09	168.07	192.53	192.69	211.62	226.14	226.95	259.47
	14	20	18	156.82	165.57	192.35	192.54	208.23	224.62	224.98	259.35
	16	20	18	155.71	163.79	192.15	192.32	206.18	223.28	223.40	259.29
	18	20	18	155.20	162.74	191.97	192.07	205.03	222.22	222.26	259.23
	20	20	18	154.98	162.23	191.83	191.83	204.40	221.53	221.53	259.18
	10	10	10	162.60	171.10	193.93	193.93	217.94	229.14	229.14	259.66
	10	10	12	162.41	170.78	193.50	193.50	217.72	228.94	228.94	259.61
	10	10	14	162.17	170.35	193.04	193.04	217.65	228.71	228.71	259.58
	10	10	16	161.89	169.88	192.63	192.63	217.62	228.50	228.50	259.56
	10	10	18	161.58	169.39	192.31	192.31	217.61	228.31	228.31	259.54
	10	12	18	159.19	167.58	191.99	192.10	214.12	226.77	227.33	259.44
	10	14	18	157.80	166.52	191.69	191.85	211.75	225.64	226.51	259.36
∞	10	16	18	157.13	165.75	191.47	191.56	210.51	224.86	225.83	259.32
	10	18	18	156.70	165.36	191.32	191.32	209.77	224.37	225.31	259.28
	10	20	18	156.46	165.12	191.10	191.21	209.42	224.10	224.98	259.25
	12	20	18	154.57	162.93	190.90	191.05	206.44	222.58	222.88	259.17
	14	20	18	153.69	161.44	190.68	190.84	204.72	221.25	221.27	259.11
	16	20	18	153.27	160.60	190.51	190.62	203.74	220.17	220.24	259.05
	18	20	18	153.06	160.16	190.37	190.43	203.27	219.52	219.53	258.99
	20	20	18	152.88	159.96	190.27	190.27	203.00	219.12	219.12	258.93

boundary conditions:

- for the SF shell

$$U|_{\xi=\xi_e,\eta=\eta_e} = 0, \quad V|_{\xi=\xi_e,\eta=\eta_e} = 0, \quad W|_{\xi=\xi_e,\eta=\eta_e} = 0 \tag{16a–16c}$$

$$\left.\frac{\partial W}{\partial n_r}\right|_{\xi=\xi_e,\eta=\eta_e} \neq 0 \tag{16d}$$

- for the CF shell

$$U|_{\xi=\xi_e,\eta=\eta_e} = 0, \quad V|_{\xi=\xi_e,\eta=\eta_e} = 0, \quad W|_{\xi=\xi_e,\eta=\eta_e} = 0 \tag{17a–17c}$$

$$\left.\frac{\partial W}{\partial n_r}\right|_{\xi=\xi_e,\eta=\eta_e} = 0, \tag{17d}$$

Table 2(a). Comparison of frequencies (in hertz) for the fully clamped aluminium cylindrical (singly-curved) shallow shell without cutout ($R_x = \infty$, $a'/a = b'/b = 0$)

$E = 10^7$ $\mathrm{lb_f/in^2}$, $\rho = 0.096$ $\mathrm{lb_m/in^2}$, $\nu = 0.33$, $R_y = 30.0$ in, $h = 0.013$ in, $a = 3.0$ in, $b = 4.0$ in

Reference	Mode sequence number									
	1	2	3	4	5	6	7	8	9	10
Experiment (Deb Nath, 1969)	814	940	1260	1306	1452	1802	1770	2100	2225	2280
ERR (Webster, 1968)	870	958	1288	1364	1440	1753	1795	2057	2220	2300
FET (Olson and Lindberg, 1971)	870	958	1288	1363	1440	1756	1780	2056	2222	2295
FER (Deb Nath, 1969)	890	973	1311	1371	1454	1775	1816	2068	2234	2319
K (Deb Nath and Petyt, 1969)	890	966	1295	1375	1450	1745	—	—	—	—
FSM (Cheung *et al.*, 1989)	874	963	1298	1369	—	—	—	—	—	—
pb-2 method ($n_1 = 10$)	870.12	958.34	1288.7	1364.1	1440.3	1753.9	1780.0	2056.5	2219.2	2289.7
pb-2 method ($n_1 = \infty$)	870.10	958.21	1288.6	1364.0	1440.2	1753.7	1779.9	2056.4	2218.9	2289.2

Table 2(b). Comparison of frequencies $\omega a^2\sqrt{(\rho h/D)}$ for the completely free shallow shells of rectangular planform without cutout ($a/h = 100$ and $a'/a = b'/b = 0$) where the *pb*-2 solution employs a super-elliptical shell with $n_1 \doteq 10$

a/b	ν	R_x/R_y	a/R_x	Reference	Mode sequence SS-1	SS-2	SA-1	SA-2	AS-1	AS-2	AA-1	AA-2
				Leissa (1973b)	19.789	24.432	35.024	61.526	35.024	61.526	13.489	—
		—	0	Gorman (1978)	19.60	24.27	34.80	61.08	34.80	61.08	13.47	—
				Leissa and Narita (1984)	19.596	24.271	34.801	61.111	34.801	61.111	13.468	69.279
				pb-2 method	19.523	24.381	34.947	61.255	34.947	61.255	13.523	69.268
			0.2	Leissa and Narita (1984)	24.741	52.574	36.957	77.063	36.957	77.063	13.462	77.647
		−1		*pb*-2 method	24.851	52.563	37.145	77.217	37.145	77.217	13.517	78.325
			0.5	Leissa and Narita (1984)	25.695	64.262	38.923	103.77	38.923	103.77	13.425	79.401
				pb-2 method	25.781	64.577	39.131	104.16	39.131	104.16	13.481	80.055
1	0.3		0.2	Leissa and Narita (1984)	21.904	38.473	34.852	75.298	37.643	61.154	13.483	70.952
		0		*pb*-2 method	21.942	38.640	35.003	75.552	37.807	61.283	13.539	70.965
			0.5	Leissa and Narita (1984)	22.074	54.329	34.870	98.220	48.711	61.326	13.508	72.479
				pb-2 method	22.119	54.697	35.029	98.412	48.939	61.391	13.564	72.533
			0.2	Leissa and Narita (1984)	19.757	42.353	35.880	73.890	35.880	73.890	13.524	69.598
		1		*pb*-2 method	19.755	42.675	36.013	74.172	36.013	74.172	13.580	69.573
			0.5	Leissa and Narita (1984)	19.997	49.623	36.862	87.725	36.862	87.725	13.576	70.723
				pb-2 method	19.988	49.974	36.994	87.875	36.994	87.875	13.633	70.635
				Gorman (1978)	19.22	24.42	34.23	60.92	34.23	60.92	13.17	68.12
	0.333	—	0	Leissa and Narita (1984)	19.224	24.423	34.233	60.951	34.233	60.951	13.169	68.142
				pb-2 method	19.224	24.535	34.376	61.099	34.376	61.099	13.223	68.132
				Gorman (1978)	21.25	87.62	57.34	158.2	59.07	103.3	25.97	99.92
2	0.333	—	0	Leiss and Narita (1984)	21.241	87.696	57.350	169.28	59.087	103.27	25.974	99.938
				pb-2 method	21.284	87.795	57.610	158.77	59.150	103.80	26.075	100.37

where ξ_e and η_e are the circumferential coordinates and n_r is the direction normal to the circumference in the xy-plane.

Accordingly, the power to the basic functions for the transverse deflection ($\alpha = w$) is set to 0, 1 or 2 corresponding to a free, simply supported or clamped edge. For the in-plane deflections ($\alpha = u$ and v), the power is set to zero for a free edge and one for either a simply supported or clamped edge. The in-plane deflection gradients are always non-zero ($\partial u/\partial n_r \neq 0$, $\partial u/\partial n_s \neq 0$, $\partial v/\partial n_r \neq 0$ and $\partial v/\partial n_s \neq 0$, where n_r and n_s are the directions normal and tangential to the outer and inner peripheries of shells) regardless of the boundary constraints.

For the doubly-connected super-elliptical shell, the basic functions can be represented by

$$\phi_1^\alpha = [(2\xi)^{2n_1} + (2\eta)^{2n_1} - 1]^{\gamma_1^\alpha}\left[\left(\frac{2a\xi}{a'}\right)^{2n_2} + \left(\frac{2b\eta}{b'}\right)^{2n_2} - 1\right]^{\gamma_2^\alpha} \tag{18}$$

$$n_1, n_2 = 1, 2, 3, \ldots, \infty, \quad \alpha = u, v \text{ and } w,$$

where $\gamma_1^\alpha = 1$ or 2 and $\gamma_2^\alpha = 0$ corresponding to the SF or CF shell. The integers n_1 and n_2 are the powers for the outer and inner super-elliptical functions. For shells having a rectangular outer boundary ($n_1 = \infty$) and a super-elliptical inner periphery, the basic functions are

$$\phi_1^\alpha = [(\xi^2 - 0.25)(\eta^2 - 0.25)]^{\gamma_1^\alpha}\left[\left(\frac{2a\xi}{a'}\right)^{2n_2} + \left(\frac{2b\eta}{b'}\right)^{2n_2} - 1\right]^{\gamma_2^\alpha} \tag{19}$$

$$n_1, n_2 = 1, 2, 3, \ldots, \infty, \quad \alpha = u, v \text{ and } w,$$

where $\gamma_1^\alpha = 1$ or 2 and $\gamma_2^\alpha = 0$ as explained earlier.

The two-dimensional polynomial $\Sigma_{i=1}^{m} f_i(\xi, \eta)$, as mentioned in eqn (13) can be expressed as

$$\sum_{i=1}^{m} f_i(\xi, \eta) = \sum_{q=0}^{p} \sum_{i=0}^{q} \xi^{q-i}\eta^i \tag{20}$$

with m and p related by

$$m = \frac{(p+1)(p+2)}{2}, \tag{21}$$

where p is the degree set of the two-dimensional polynomials.

3. NUMERICAL STUDIES

Convergence and comparison of eigenvalues are performed to justify the accuracy and validity of the present analysis and numerical algorithm. For descriptive purposes, two kinds of boundary conditions are studied, namely the SF shell (simply supported at the outer edge and free at the inner edge) and the CF shell (fully clamped at the outer edge and free at the inner edge). The outer periphery has super-elliptical powers $2n_1 = 2$, 10, 20 and ∞ whereas the inner cutout is circular ($2n_2 = 2$). The effect of Gaussian curvature ($1/R_xR_y$) is investigated by varying the curvature ratio (R_y/R_x). New data are presented for wide ranges of shallowness ratios (a/R_y) and curvature ratios. The Poisson ratio is fixed at $v = 0.3$, thickness ratio $a/h = 100.0$, aspect ratio $a/b = 1$, cutout ratios $a'/a = 0.3$ and $a'/b' = 1.0$.

3.1. *Convergence and comparison studies*

Since the *pb*-2 shape functions adopted are orthogonally generated two-dimensional polynomials which satisfy the geometric boundary conditions, the application of the Ritz procedure in the present analysis ensures the upper bound convergence of eigenvalue to the exact solutions. In order to determine the lowest degree of polynomial required to achieve satisfactory accuracy, convergence tests have been carried out with the results given in Tables 1(a) and 1(b). The degrees of polynomial for u, v and w for various n_1 are increased from 10 and onwards. The upper bound nature of the Ritz formulation is clearly shown in the convergence tables where the eigenvalues decrease as the polynomial degrees increase. It is found that the degrees 20, 20 and 18 for u, v and w are sufficient to furnish the acceptable accurate solutions within the engineering interest.

Table 2(a) shows the comparison of frequencies (in hertz) for a fully clamped aluminium cylindrical shallow shell without cutout. The shell geometric specifications and mechanical properties of the experimental specimen by Deb Nath (1969) are listed in the same table. Results of Petyt (1971) and the finite strip results of Cheung *et al.* (1989) are reproduced and compared to the present *pb*-2 solutions. In this comparison study, ERR refers to the extended Rayleigh–Ritz method of Webster (1968); FET, the triangular finite element method of Olson and Lindberg (1971); FER, the rectangular finite element method of Deb Nath (1969); K, the Kantorovich method of Kantorovich and Krylov (1964) which was applied by Deb Nath and Petyt (1969) and FSM, the finite strip method of Cheung *et al.* (1989). The present *pb*-2 method is used to provide two sets of solutions. The first set

Table 3(a). Frequency parameters $\lambda = \omega ab\sqrt{(\rho h/D)}$ for the doubly-connected super-elliptical ($n_1 = 1$, 5 and $n_2 = 1$) simply supported shallow shells ($\nu = 0.3$, $a/b = 1.0$, $a'/b' = 1.0$, $a'/a = 0.3$ and $a/h = 100.0$)

n_1	b/R_y	R_y/R_x	Mode sequence number 1	2	3	4	5	6	7	8
1	0.0	all	18.663	51.933	51.933	97.092	97.092	148.20	155.50	155.50
	0.1	−1.0	38.900	60.474	60.474	100.09	101.35	150.74	157.88	157.88
		−0.5	33.758	55.375	59.822	98.971	99.671	149.92	157.01	157.03
		0.0	34.404	54.189	60.171	98.582	98.871	149.97	156.80	156.81
		0.5	40.587	57.178	61.504	98.930	98.992	150.87	157.25	157.25
		1.0	50.256	63.752	63.752	100.00	100.00	152.63	158.35	158.35
	0.3	−1.0	102.28	105.71	105.71	121.28	130.05	170.24	175.09	175.09
		−0.5	77.417	84.898	102.21	112.74	116.99	164.15	167.71	168.61
		0.0	69.329	86.468	104.11	109.54	110.30	165.10	166.04	166.18
		0.5	88.275	106.47	111.16	112.16	112.72	170.05	170.14	172.37
		1.0	119.92	119.92	122.07	122.07	136.65	179.04	179.04	187.46
	0.5	−1.0	154.52	158.23	158.23	160.79	172.09	203.67	203.67	206.74
		−0.5	108.14	133.38	135.50	141.04	149.75	188.06	188.78	193.75
		0.0	91.228	120.81	127.64	137.47	152.85	179.00	184.94	197.41
		0.5	128.57	129.72	133.20	167.09	168.54	190.68	193.52	216.75
		1.0	149.08	149.08	189.81	189.81	205.83	212.29	212.29	254.29
5	0.0	all	19.109	47.625	47.626	75.059	94.274	112.40	125.24	125.24
	0.1	−1.0	39.952	56.993	56.993	79.408	97.989	116.53	127.76	127.76
		−0.5	34.581	51.286	56.445	77.865	96.472	115.20	126.37	127.53
		0.0	34.964	49.943	56.892	77.498	95.777	115.13	126.26	127.81
		0.5	40.961	53.322	58.310	78.318	96.031	116.25	127.42	128.58
		1.0	50.540	60.629	60.629	80.277	97.102	118.64	129.83	129.84
	0.3	−1.0	103.31	103.31	103.46	107.48	123.33	147.27	147.31	147.31
		−0.5	74.032	86.389	97.107	100.61	109.17	136.34	138.91	144.45
		0.0	65.432	87.386	94.296	102.09	103.12	135.14	139.62	146.51
		0.5	86.004	99.544	106.32	106.72	110.44	144.05	147.33	152.15
		1.0	111.03	116.48	121.28	121.28	132.43	161.10	161.10	167.09
	0.5	−1.0	146.20	150.52	150.52	158.12	160.90	185.65	185.65	199.51
		−0.5	104.75	125.66	126.10	135.26	136.96	169.30	172.43	182.12
		0.0	87.909	108.89	119.04	134.55	138.85	167.88	169.16	177.85
		0.5	122.66	127.44	128.13	160.61	161.07	181.04	182.83	195.27
		1.0	144.92	147.48	188.63	188.64	195.65	205.65	205.65	237.16

Table 3(b). Frequency parameters $\lambda = \omega ab\sqrt{(\rho h/D)}$ for the doubly-connected super-elliptical and rectangular ($n_1 = 10, \infty$ and $n_2 = 1$) simply supported shallow shells ($\nu = 0.3$, $a/b = 1.0$, $a'/b' = 1.0$, $a'/a = 0.3$ and $a/h = 100.0$)

			Mode sequence number							
n_1	b/R_y	R_y/R_x	1	2	3	4	5	6	7	8
	0.0	all	19.443	48.112	48.112	75.646	94.343	112.94	125.82	125.82
		−1.0	40.122	57.383	57.383	79.954	98.044	117.07	128.33	128.33
		−0.5	34.771	51.733	56.841	78.427	96.536	115.74	126.94	128.10
	0.1	0.0	35.146	50.408	57.288	78.066	95.848	115.67	126.83	128.38
		0.5	41.110	53.759	58.700	78.884	96.107	116.79	128.00	129.15
		1.0	50.655	61.008	61.008	80.833	97.183	119.18	130.40	130.40
		−1.0	103.46	103.46	103.63	107.83	123.31	147.73	147.82	147.82
		−0.5	74.321	86.533	97.527	100.76	109.25	136.89	139.35	144.96
10	0.3	0.0	65.797	87.521	94.761	102.21	103.28	135.71	140.06	147.01
		0.5	86.286	100.02	106.41	106.91	110.61	144.62	147.77	152.64
		1.0	111.49	116.66	121.47	121.47	132.68	161.63	161.63	167.40
		−1.0	146.39	150.62	150.62	158.57	160.81	185.98	185.98	199.61
		−0.5	104.96	125.94	126.14	135.61	137.15	169.63	172.77	182.34
	0.5	0.0	88.207	109.03	119.41	134.93	139.14	168.20	169.48	178.68
		0.5	122.88	127.66	128.58	161.09	161.36	181.47	183.16	196.22
		1.0	145.28	148.01	188.80	188.80	196.27	206.34	206.34	237.95
	0.0	all	19.515	47.595	47.595	75.898	94.092	113.32	125.50	125.50
		−1.0	40.020	56.865	56.865	80.172	97.763	117.40	128.02	128.02
		−0.5	34.709	51.214	56.333	78.652	96.270	116.08	126.65	127.77
	0.1	0.0	35.094	49.898	56.791	78.279	95.586	116.02	126.53	128.04
		0.5	41.034	53.269	58.217	79.068	95.832	117.13	127.69	128.81
		1.0	50.536	60.537	60.537	80.969	96.884	119.50	130.07	130.07
		−1.0	102.72	102.72	103.08	107.87	122.82	147.57	147.57	147.84
		−0.5	73.743	86.102	97.589	100.06	108.98	136.77	139.40	144.52
∞	0.3	0.0	65.295	87.098	94.728	102.01	102.65	135.57	140.09	146.52
		0.5	85.837	99.783	106.03	106.42	110.06	144.31	147.87	152.14
		1.0	110.99	116.01	120.96	120.96	132.07	161.05	161.05	167.52
		−1.0	146.23	149.42	149.42	157.46	159.96	185.83	185.83	199.50
		−0.5	104.21	125.80	125.88	134.52	136.25	169.56	172.23	181.22
	0.5	0.0	87.633	108.89	119.04	133.79	138.41	166.73	169.26	177.11
		0.5	122.27	127.12	127.79	159.94	160.52	180.95	182.04	194.13
		1.0	144.05	146.73	188.10	188.10	195.14	204.74	204.74	235.96

of solutions is obtained by assigning $n_1 = 10$ which is in close resemblance with a rectangular cylindrical shell as shown in Fig. 1. The second set of solutions ($n_1 = \infty$) is for the rectangular shell.

The implication of comparison shown in Table 2(a) is two-fold and far-reaching. Firstly, it demonstrates the reliability of the present method of analysis with respect to a variety of other computational solutions as well as the experimental results of Deb Nath (1969). Close agreement between the various methods has been observed especially between the solutions of ERR (Webster, 1968), FET (Olson and Lindberg, 1971) and the present *pb*-2 method. Secondly, it provides the confirmation of analytical and numerical consistency that the results for super-elliptical shells with a high super-elliptical power ($n_1 \geqslant 10$) approach the rectangular shell solutions.

Table 2(b) further compares the solutions of a free shallow shell of rectangular planform with various other sources. The flat plate results ($a/R_x = 0$) of Leissa (1973b) and Gorman (1978) are also included. SS-1 and SS-2 denote the first and second symmetric–symmetric modes with respect to the x- and y-axis. SA, AS and AA are the corresponding symmetric–antisymmetric, antisymmetric–symmetric and antisymmetric–antisymmetric modes. The results of the present *pb*-2 method are generated using a super-elliptical shell model with $n_1 = 10$. The non-dimensional frequency parameter presented here is expressed in terms of $\omega a^2\sqrt{(\rho h_0/D_0)}$. Good agreement between the results is again achieved. Consequently, we can conclude that a super-elliptical shell model with a high super-elliptical power ($n_1 \geqslant 10$) can well simulate a rectangular shell so far as its vibratory characteristics are concerned.

3.2. *Results and discussion*

New sets of data for selective shell configurations are presented in Tables 3(a), 3(b), 4(a) and 4(b). Tables 3(a) and 3(b) show the non-dimensional frequency parameter $\lambda = \omega ab\sqrt{(\rho h_0/D_0)}$ for a simply supported shallow shell with various outer super-elliptical powers $n_1 = 1$, 5, 10 and ∞ and a circular cutout $n_2 = 1$. Tables 4(a) and 4(b) present the corresponding data for a fully clamped shallow shell. For all cases, the shallowness ratio b/R_y ranges from 0.0 to 0.5 and the curvature ratio R_y/R_x from -0.5 to 0.5. A negative curvature ratio represents a hyperbolic paraboloidal shell whereas a positive R_y/R_x represents a spherical shell.

Note that cases where $b/R_y \neq 0$ and $R_y/R_x = 0$ correspond to cylindrical shells with shallowness ratio $a/R_x = 0$. Furthermore, λ is completely independent of the curvature ratio for $b/R_y = 0$ and $R_y/R_x \ll \infty$ because it corresponds to a flat plate with infinite radii of curvature. The consistency of results for $n_1 = 10$ and $n_1 = \infty$ as exemplified clearly in the previous section is again observed here for both simply supported and fully clamped shells [see Tables 3(b) and 4(b)].

In Tables 3(a) and 3(b), it is observed that the fundamental frequencies increase significantly for deeper shells (higher b/R_y) having the same boundary conditions. For example, the fundamental λ ($n_1 = 1$ and $R_y/R_x = -1.0$) increases from 38.900 for

Table 4(a). Frequency parameters $\lambda = \omega ab\sqrt{(\rho h/D)}$ for the doubly-connected super-elliptical ($n_1 = 1$, 5 and $n_2 = 1$) fully clamped shallow shells ($\nu = 0.3$, $a/b = 1.0$, $a'/b' = 1.0$, $a'/a = 0.3$ and $a/h = 100.0$)

n_1	b/R_y	R_y/R_x	Mode sequence number							
			1	2	3	4	5	6	7	8
	0.0	all	45.699	78.728	78.731	131.37	131.38	197.13	197.13	207.00
		−1.0	55.884	83.910	83.913	133.25	134.04	198.71	198.72	208.82
		−0.5	52.815	80.707	83.603	132.53	132.98	198.13	198.13	208.24
	0.1	0.0	53.140	80.049	83.921	132.26	132.46	197.97	197.97	208.31
		0.5	56.813	82.006	84.863	132.43	132.48	198.23	198.23	209.02
		1.0	63.229	86.398	86.402	133.04	133.04	198.91	198.91	210.38
		−1.0	105.80	116.97	116.97	147.31	153.50	210.71	210.71	223.01
		−0.5	90.735	94.984	114.88	141.40	144.78	205.64	205.92	218.21
1	0.3	0.0	89.738	92.055	117.00	139.04	140.23	204.26	204.34	218.97
		0.5	104.42	109.77	123.13	140.44	140.68	206.59	206.61	225.06
		1.0	132.46	132.46	136.84	145.37	145.38	212.30	212.30	236.68
		−1.0	161.64	162.32	162.32	171.64	185.63	232.14	232.14	249.61
		−0.5	118.11	134.82	157.27	157.38	164.32	219.68	220.32	238.18
	0.5	0.0	105.72	134.26	151.13	154.05	161.70	215.26	216.27	240.86
		0.5	138.06	152.03	154.57	169.86	174.94	221.38	221.99	256.60
		1.0	166.17	166.18	193.48	193.48	211.81	235.44	235.44	287.19
	0.0	all	39.433	71.310	71.312	104.16	125.67	156.63	162.17	162.18
		−1.0	51.603	77.184	77.185	106.70	128.10	159.56	163.84	163.85
		−0.5	47.947	73.448	76.936	105.77	127.13	158.59	162.93	163.68
	0.1	0.0	48.098	72.635	77.309	105.51	126.68	158.55	162.86	163.86
		0.5	52.037	74.858	78.292	105.92	126.79	159.42	163.62	164.37
		1.0	58.976	79.860	79.861	106.98	127.42	161.21	165.20	165.21
		−1.0	105.51	112.79	112.79	124.98	145.85	176.98	176.99	182.10
		−0.5	88.610	89.585	111.20	117.76	136.84	169.44	174.86	175.10
5	0.3	0.0	82.353	90.090	113.65	115.55	132.28	168.65	175.15	176.50
		0.5	98.609	107.36	118.62	119.84	134.28	174.79	180.52	181.70
		1.0	126.28	128.98	128.95	133.75	140.31	186.93	186.94	196.10
		−1.0	154.29	157.57	157.57	160.74	175.25	202.83	202.84	223.63
		−0.5	112.58	135.24	138.01	151.19	151.73	186.92	195.24	207.19
	0.5	0.0	98.452	132.46	134.82	138.91	156.47	185.00	197.82	208.71
		0.5	133.42	138.94	145.96	164.01	172.15	196.64	206.42	224.10
		1.0	154.53	161.77	191.51	191.51	203.91	220.90	220.90	259.38

Table 4(b). Frequency parameters $\lambda = \omega ab\sqrt{(\rho h/D)}$ for the doubly-connected super-elliptical and rectangular ($n_1 = 10$, ∞ and $n_2 = 1$) fully clamped shallow shells ($\nu = 0.3$, $a/b = 1.0$, $a'/b' = 1.0$, $a'/a = 0.3$ and $a/h = 100.0$)

			Mode sequence number							
n_1	b/R_y	R_y/R_x	1	2	3	4	5	6	7	8
	0.0	all	39.458	71.721	71.722	104.12	125.84	156.33	162.18	162.18
		−1.0	51.660	77.580	77.581	106.67	128.26	159.28	163.85	163.85
		−0.5	47.993	73.852	77.332	105.74	127.29	158.30	162.94	163.69
	0.1	0.0	48.140	73.041	77.701	105.48	126.84	158.26	162.87	163.87
		0.5	52.082	75.255	78.680	105.90	126.96	159.13	163.63	164.38
		1.0	59.030	80.242	80.243	106.97	127.60	160.93	165.23	165.23
		−1.0	105.70	113.15	113.15	124.98	145.99	176.99	176.99	181.94
		−0.5	88.987	89.741	111.56	117.76	136.96	169.41	174.68	175.15
10	0.3	0.0	82.728	90.237	114.00	115.59	132.41	168.65	174.96	176.59
		0.5	98.946	107.52	118.72	120.17	134.49	174.86	180.66	181.51
		1.0	126.46	129.26	129.26	133.96	140.59	187.14	187.14	195.90
		−1.0	154.33	157.95	157.95	161.12	175.36	202.85	202.85	223.62
		−0.5	112.95	135.57	138.05	151.25	152.07	186.88	195.35	207.15
	0.5	0.0	98.805	132.59	135.27	138.89	156.79	185.04	198.01	208.64
		0.5	133.73	139.21	146.25	164.38	172.49	196.88	206.80	223.95
		1.0	154.98	162.23	191.83	191.83	204.40	221.53	221.53	259.18
	0.0	all	39.360	69.417	69.418	103.57	124.72	156.15	160.47	160.47
		−1.0	51.470	75.364	75.364	106.12	127.11	159.09	162.19	162.19
		−0.5	47.833	71.580	75.124	105.18	126.15	158.11	161.28	161.99
	0.1	0.0	47.988	70.766	75.514	104.91	125.70	158.07	161.20	162.16
		0.5	51.917	73.039	76.524	105.30	125.81	158.94	161.97	162.68
		1.0	58.833	78.127	78.127	106.34	126.43	160.73	163.56	163.56
		−1.0	105.09	111.08	111.08	124.41	144.63	175.62	175.62	181.70
		−0.5	86.856	89.233	109.55	117.16	135.77	168.08	173.50	174.36
∞	0.3	0.0	80.615	89.731	112.10	114.87	131.27	167.29	174.61	174.87
		0.5	97.119	106.98	117.80	118.42	133.17	173.38	178.99	181.20
		1.0	125.28	127.63	127.63	133.29	139.02	185.50	185.50	195.64
		−1.0	153.68	155.53	155.53	159.91	173.61	201.98	201.98	223.40
		−0.5	110.86	134.45	137.35	149.69	150.04	186.23	193.82	206.66
	0.5	0.0	96.819	131.59	133.52	138.31	154.56	184.25	196.66	208.06
		0.5	132.13	137.72	144.57	163.21	170.58	195.51	205.13	223.59
		1.0	152.88	159.96	190.27	190.27	203.00	219.12	219.12	258.93

$b/R_y = 0.1$ to 154.54 for $b/R_y = 0.5$ in Table 3(a). The similar characteristic can also be observed in Tables 4(a) and 4(b). The fully clamped shells also provide a relatively higher fundamental λ with respect to the simply supported shell. The effect of R_y/R_x on the fundamental λ can be readily seen in the tables where it initially decreases and then increases when R_y/R_x changes from -1 to 1. The lowest fundamental λ generally corresponds to a negative R_y/R_x.

A set of selected vibration mode shapes is also included for illustrative purposes. Figures 2(a) and 2(b) illustrate the vibration mode shapes of simply supported super-elliptical shells having $n_1 = 1$ and 10 ($\nu = 0.3$, $a/b = 1$, $a'/a = 0.3$, $a'/b' = 1$, $a/h = 100$ and $n_2 = 1$) with a free circular cutout. Figures 3(a) and 3(b) are the corresponding mode shapes of a fully clamped shell at the outer edge. The shaded regions represent negative deflection amplitudes and the unshaded regions otherwise. The lines of demarcation are the nodal lines having zero deflection. It is clear that these modes can be classified into SS, SA, AS and AA modes with respect to the x- and y-axis. There are more nodal lines for higher modes of vibration as demonstrated in these figures.

4. CONCLUSIONS

A global continuum approach for free vibration of perforated doubly-curved shallow shells with rounded corners has been presented. The outer and cutout peripheries of a shell were described by super-elliptical functions having different powers. The analysis accounts

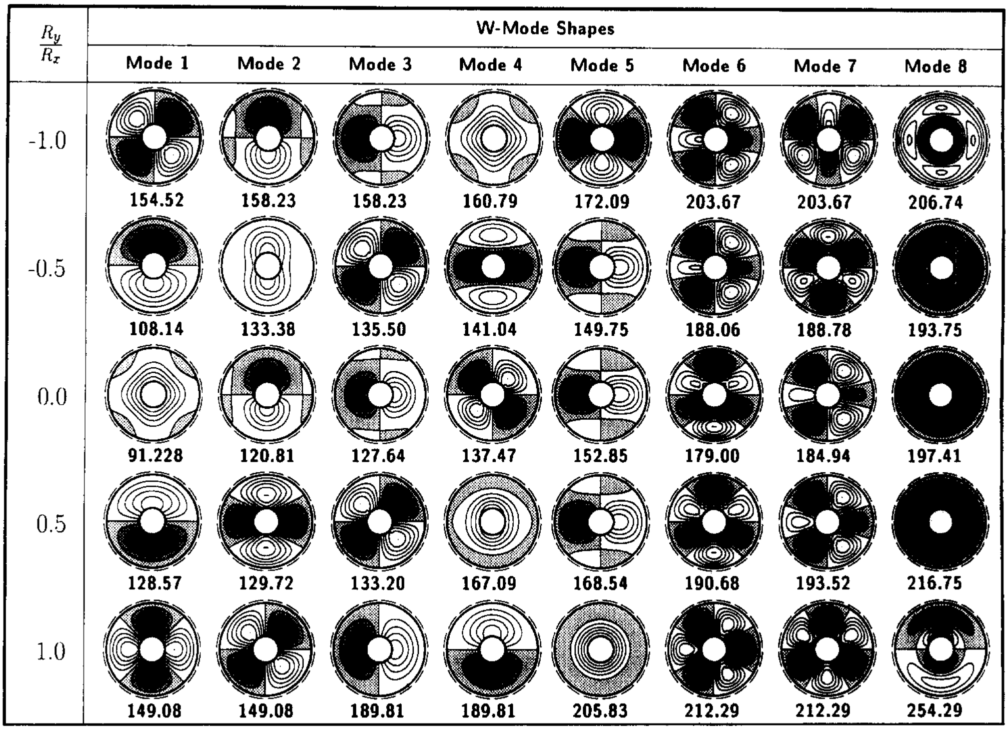

Fig. 2(a). Vibration mode shapes for a doubly-connected simply supported circular shell with a completely free circular cutout ($\nu = 0.3$, $a/b = 1.0$, $a'/b' = 1.0$, $a'/a = 0.3$, $b/h = 100.0$, $b/R_y = 0.5$ and $n_1 = n_2 = 1$).

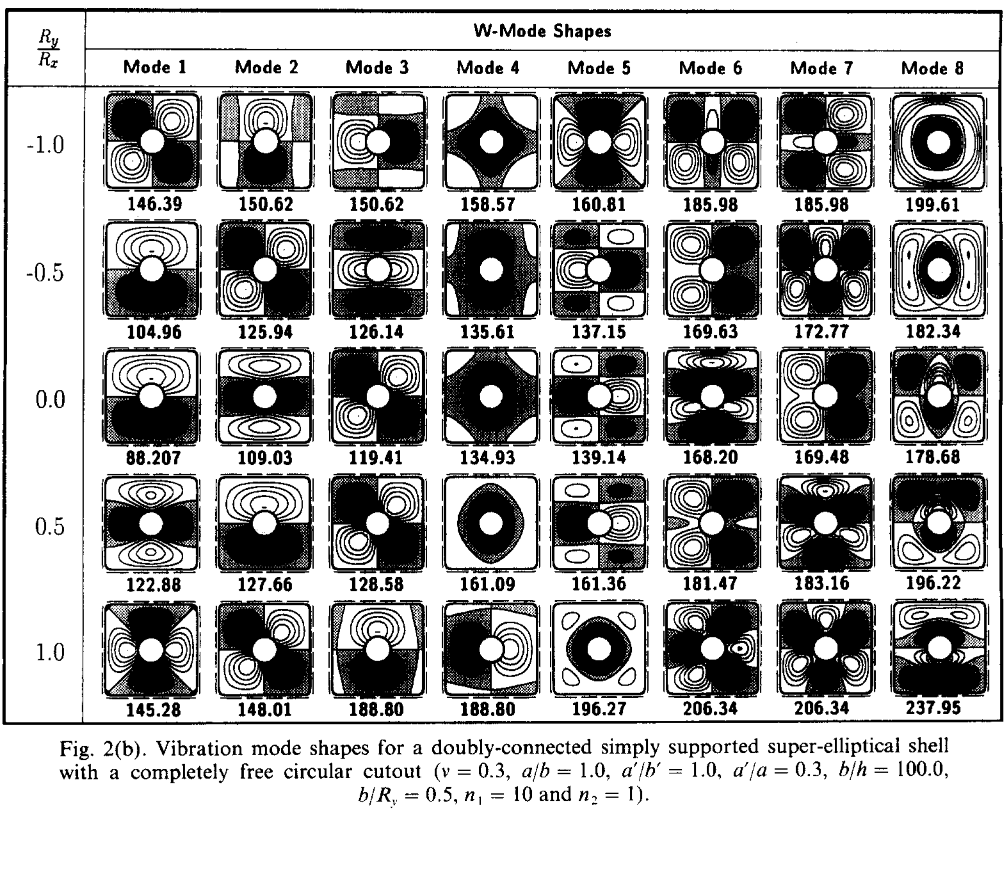

Fig. 2(b). Vibration mode shapes for a doubly-connected simply supported super-elliptical shell with a completely free circular cutout ($\nu = 0.3$, $a/b = 1.0$, $a'/b' = 1.0$, $a'/a = 0.3$, $b/h = 100.0$, $b/R_y = 0.5$, $n_1 = 10$ and $n_2 = 1$).

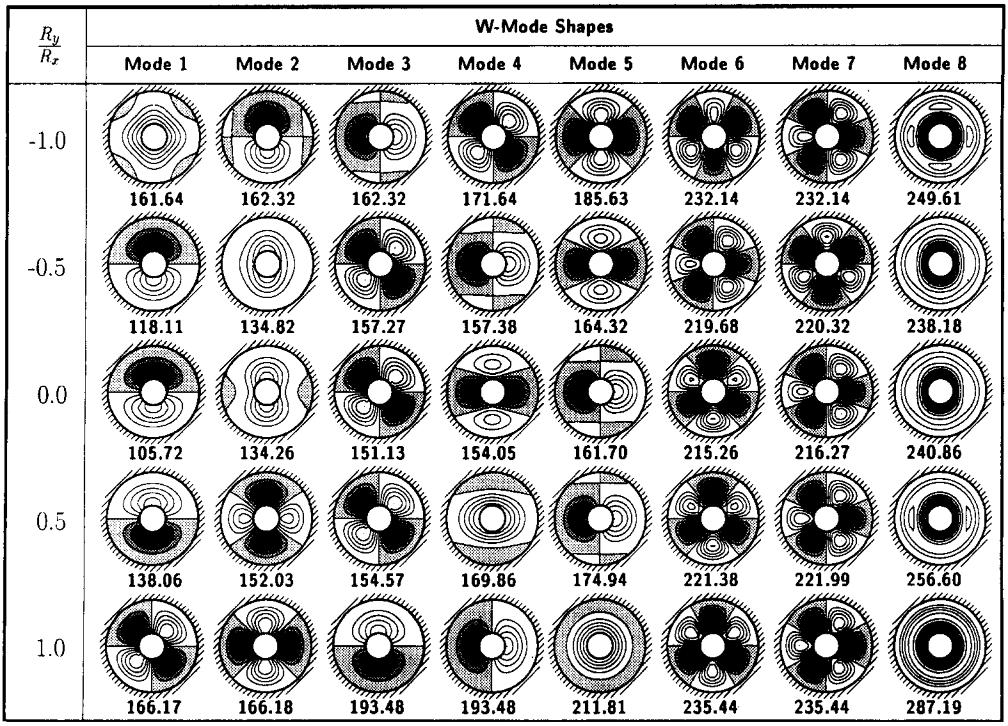

Fig. 3(a). Vibration mode shapes for a doubly-connected fully clamped circular shell with a completely free circular cutout ($\nu = 0.3$, $a/b = 1.0$, $a'/b' = 1.0$, $a'/a = 0.3$, $b/h = 100.0$, $b/R_y = 0.5$ and $n_1 = n_2 = 1$).

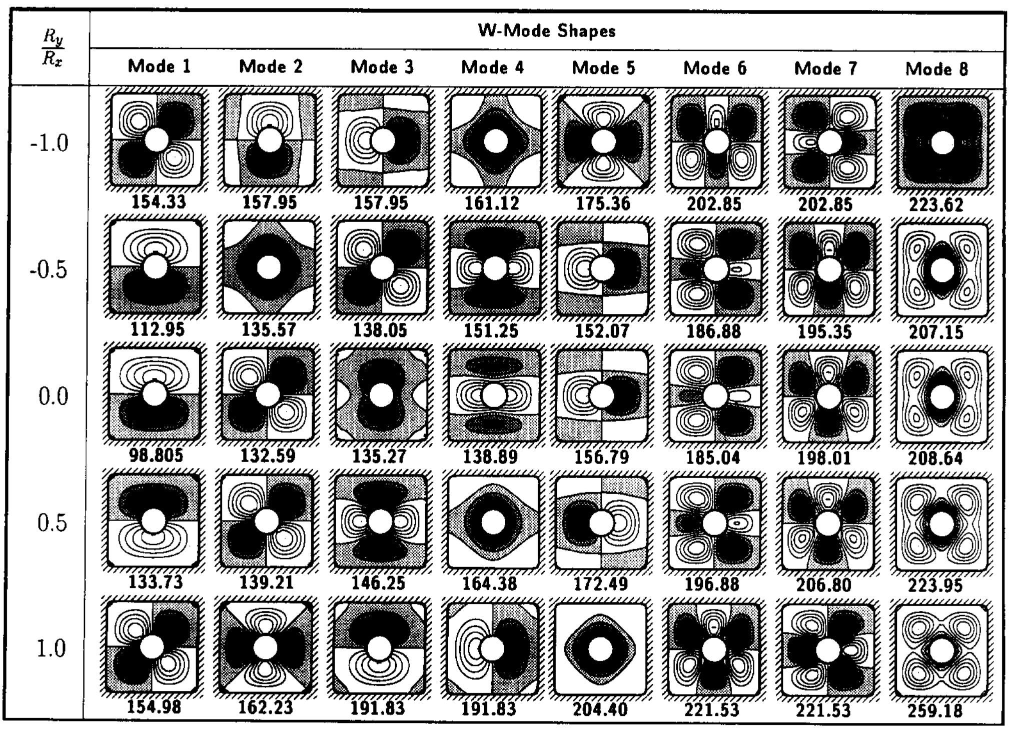

Fig. 3(b). Vibration mode shapes for a doubly-connected fully clamped super-elliptical shell with a completely free circular cutout ($\nu = 0.3$, $a/b = 1.0$, $a'/b' = 1.0$, $a'/a = 0.3$, $b/h = 100.0$, $b/R_y = 0.5$, $n_1 = 10$ and $n_2 = 1$).

for general types of boundary constraints. The *pb*-2 shape functions adopted are sets of orthogonally generated two-dimensional polynomials. These admissible shape functions are kinematically oriented and satisfy the geometric boundary conditions at the outset.

A comprehensive convergence study has been performed to demonstrate the upper bound eigenvalues and to determine the degrees of polynomial required to ensure a satisfactory convergence. Comparison of frequencies with other experimental and computational results has also been presented. Selected numerical examples included are the simply supported and fully clamped shells (the outer peripheries) with a free, circular inner cutout. The effects of outer super-elliptical power (n_1), shallowness ratio and curvature ratio (which determines whether a shell is hyperbolic paraboloidal, cylindrical or spherical) have been carefully examined. It has been shown that the natural frequencies of a super-elliptical shell with a high outer super-elliptical power approach the solutions of a rectangular shell having the same geometrical and mechanical properties [see Sections 3.1 and 3.2 or Tables 2, 3(b) and 4(b)]. It has also been justified in the numerical studies that a minimum fundamental frequency exists corresponding to a shell with a negative curvature ratio (a hyperbolic paraboloidal shell).

REFERENCES

Cheung, Y. K., Li, W. Y. and Tham, L. G. (1989). Free vibration analysis of singly curved shell by spline finite strip method. *J. Sound Vibr.* **128,** 411–422.

Deb Nath, J. M. (1969). Dynamics of rectangular curved plates. Ph.D. thesis, University of Southampton.

Deb Nath, J. M. and Petyt, M. (1969). Institute of Sound and Vibration Research Technical Report No. 19. Application of the method of Kantorovich to the solution of problems of free vibration of singly curved rectangular plates including the presence of membrane stresses.

Gorman, D. J. (1978). Free vibration analysis of the completely free rectangular plate by the method of superposition. *J. Sound Vibr.* **57,** 437–447.

Irie, T., Yamada, G. and Sonoda, M. (1983). Natural frequencies of square membrane and square plate with rounded corners. *J. Sound Vibr.* **86,** 442–448.

Kantorovich, L. V. and Krylov, I. V. (1964). *Approximate Methods of Higher Analysis*. Interscience, New York.

Leissa, A. W. (1973a). Vibration of shells, NASA SP-288.

Leissa, A. W. (1973b). The free vibration of rectangular plates. *J. Sound Vibr.* **31,** 257–259.

Leissa, A. W., Lee, J. K. and Wang, A. J. (1983). Vibration of cantilevered doubly-curved shallow shells. *Int. J. Solids Structures* **19,** 411–424.

Leissa, A. W. and Narita, Y. (1984). Vibrations of completely free shallow shells of rectangular planform. *J. Sound Vibr.* **96,** 207–218.

Liew, K. M. (1993). Treatment of over-restrained boundaries for doubly connected plates of arbitrary shape in vibration analysis. *Int. J. Solids Structures* **30,** 337–347.

Liew, K. M. and Lim, C. W. (1994a). Vibratory characteristics of cantilevered rectangular shallow shells of variable thickness. *AIAA J.*, to be published.

Liew, K. M. and Lim, C. W. (1994b). Flexural vibration of doubly-curved shallow shells. *Acta Mech.*, to be published.

Lim, C. W. and Liew, K. M. (1994). A *pb*-2 Ritz formulation for flexural vibration of shallow cylindrical shells of rectangular planform. *J. Sound Vibr.*, to be published.

Narita, Y. and Leissa, A. W. (1986). Vibrations of completely free shallow shells of curvilinear planform. *ASME J. appl. Mech.* **53,** 647–651.

Olson, M. D. and Lindberg, G. M. (1971). Dynamic analysis of shallow shell with a doubly-curved triangular finite element. *J. Sound Vibr.* **19,** 299–318.

Petyt, M. (1971). Vibration of curved plates. *J. Sound Vibr.* **15,** 381–395.

Wang, C. M., Wang, L. and Liew, K. M. (1993). Vibration and buckling of super-elliptical plates. *J. Sound Vibr.*, to be published.

Webster, J. J. (1968). Free vibrations of rectangular curved panels. *Int. J. Mech. Sci.* **10,** 571–582.

APPENDIX A

Minimization of the energy expressions as given in eqn (11) is described as follows:

$$\frac{\partial(\mathscr{U}_s)_{\max}}{\partial C_i^u} = \frac{12abD}{h^2}\left[\frac{1}{a^2}\sum_{j=1}^{m} C_j^u \mathscr{I}_{uiuj}^{1010} + \frac{\nu}{ab}\sum_{j=1}^{m} C_j^v \mathscr{I}_{uivj}^{1001} + \frac{1}{a}\left(\frac{1}{R_x}+\frac{\nu}{R_y}\right)\sum_{j=1}^{m} C_j^w \mathscr{I}_{uiwj}^{1000} + \frac{1-\nu}{2}\left(\frac{1}{b^2}\sum_{j=1}^{m} C_j^u \mathscr{I}_{uiuj}^{0101} + \frac{1}{ab}\sum_{j=1}^{m} C_j^v \mathscr{I}_{uivj}^{0110}\right)\right] \quad \text{(A1)}$$

$$\frac{\partial(\mathscr{U}_s)_{\max}}{\partial C_i^v} = \frac{12abD}{h^2}\left[\frac{\nu}{ab}\sum_{j=1}^{m} C_j^u \mathscr{I}_{uiuj}^{0110} + \frac{1}{b^2}\sum_{j=1}^{m} C_j^v \mathscr{I}_{viuj}^{0101} + \frac{1}{b}\left(\frac{\nu}{R_x}+\frac{\nu}{R_y}\right)\sum_{j=1}^{m} C_j^w \mathscr{I}_{viwj}^{0100} + \frac{1-\nu}{2}\left(\frac{1}{ab}\sum_{j=1}^{m} C_j^u \mathscr{I}_{viuj}^{1001} + \frac{1}{a^2}\sum_{j=1}^{m} C_j^v \mathscr{I}_{vivj}^{1010}\right)\right] \tag{A2}$$

$$\frac{\partial(\mathscr{U}_s)_{\max}}{\partial C_i^w} = \frac{12abD}{h^2}\left[\frac{1}{a}\left(\frac{1}{R_x}+\frac{\nu}{R_y}\right)\sum_{j=1}^{m} C_j^u \mathscr{I}_{wiuj}^{0010} + \frac{1}{b}\left(\frac{\nu}{R_x}+\frac{1}{R_y}\right)\sum_{j=1}^{m} C_j^v \mathscr{I}_{wivj}^{0001} + \left(\frac{1}{R_x^2}+\frac{2\nu}{R_xR_y}+\frac{1}{R_y^2}\right)\sum_{j=1}^{m} C_j^w \mathscr{I}_{wiwj}^{0000}\right] \tag{A3}$$

$$\frac{\partial(\mathscr{U}_b)_{\max}}{\partial C_i^u} = 0 \tag{A4}$$

$$\frac{\partial(\mathscr{U}_b)_{\max}}{\partial C_i^v} = 0 \tag{A5}$$

$$\frac{\partial(\mathscr{U}_b)_{\max}}{\partial C_i^w} = \frac{D}{ab}\left[\left(\frac{b}{a}\right)^2\sum_{j=1}^{m} C_j^w \mathscr{I}_{wiwj}^{2020} + \left(\frac{a}{b}\right)^2\sum_{j=1}^{m} C_j^w \mathscr{I}_{wiwj}^{0202} + \nu\left(\sum_{j=1}^{m} C_j^w \mathscr{I}_{wiwj}^{0220} + \sum_{j=1}^{m} C_j^w \mathscr{I}_{wiwj}^{2002}\right) + 2(1-\nu)\sum_{j=1}^{m} C_j^w \mathscr{I}_{wiwj}^{1111}\right] \tag{A6}$$

and

$$\frac{\partial \mathscr{T}_{\max}}{\partial C_i^\alpha} = \rho h\omega^2 ab\sum_{j=1}^{m} C_j^\alpha \mathscr{I}_{\alpha i\alpha j}^{0000}; \quad \alpha = u, v \text{ and } w, \tag{A7}$$

where

$$\mathscr{I}_{uiuj}^{defg} = \iint_A \frac{\partial^{d+e}\phi_i^u(\xi,\eta)}{\partial\xi^d\,\partial\eta^e}\frac{\partial^{f+g}\phi_j^u(\xi,\eta)}{\partial\xi^f\,\partial\eta^g}\,\mathrm{d}\xi\,\mathrm{d}\eta \tag{A8}$$

$$\mathscr{I}_{uivj}^{defg} = \iint_A \frac{\partial^{d+e}\phi_i^u(\xi,\eta)}{\partial\xi^d\,\partial\eta^e}\frac{\partial^{f+g}\phi_j^v(\xi,\eta)}{\partial\xi^f\,\partial\eta^g}\,\mathrm{d}\xi\,\mathrm{d}\eta \tag{A9}$$

$$\mathscr{I}_{uiwj}^{defg} = \iint_A \frac{\partial^{d+e}\phi_i^u(\xi,\eta)}{\partial\xi^d\,\partial\eta^e}\frac{\partial^{f+g}\phi_j^w(\xi,\eta)}{\partial\xi^f\,\partial\eta^g}\,\mathrm{d}\xi\,\mathrm{d}\eta \tag{A10}$$

$$\mathscr{I}_{vivj}^{defg} = \iint_A \frac{\partial^{d+e}\phi_i^v(\xi,\eta)}{\partial\xi^d\,\partial\eta^e}\frac{\partial^{f+g}\phi_j^v(\xi,\eta)}{\partial\xi^f\,\partial\eta^g}\,\mathrm{d}\xi\,\mathrm{d}\eta \tag{A11}$$

$$\mathscr{I}_{viwj}^{defg} = \iint_A \frac{\partial^{d+e}\phi_i^v(\xi,\eta)}{\partial\xi^d\,\partial\eta^e}\frac{\partial^{f+g}\phi_j^w(\xi,\eta)}{\partial\xi^f\,\partial\eta^g}\,\mathrm{d}\xi\,\mathrm{d}\eta \tag{A12}$$

$$\mathscr{I}_{wiwj}^{defg} = \iint_A \frac{\partial^{d+e}\phi_i^w(\xi,\eta)}{\partial\xi^d\,\partial\eta^e}\frac{\partial^{f+g}\phi_j^w(\xi,\eta)}{\partial\xi^f\,\partial\eta^g}\,\mathrm{d}\xi\,\mathrm{d}\eta \tag{A13}$$

and $i, j = 1, 2, \ldots m$. The double integrations above are symmetric and in general $\mathscr{I}_{\alpha i\beta j}^{defg} = \mathscr{I}_{\beta j\alpha i}^{fgde}$.

APPENDIX B

The stiffness and mass matrices as given in eqn (12) are

$$\mathbf{K} = \begin{bmatrix} [K_{uu}] & [K_{uv}] & [K_{uw}] \\ & [K_{vv}] & [K_{vw}] \\ \text{sym.} & & [K_{ww}] \end{bmatrix} \tag{B1}$$

$$\mathbf{M} = \begin{bmatrix} [M_{uu}] & [0] & [0] \\ & [M_{vv}] & [0] \\ \text{sym.} & & [M_{ww}] \end{bmatrix} \tag{B2}$$

and the vector of unknown coefficients is

$$\{\mathbf{C}\} = \begin{Bmatrix} \{C_u\} \\ \{C_v\} \\ \{C_w\} \end{Bmatrix}. \tag{B3}$$

The elements in eqns (B1) and (B2) can be expressed as

$$K_{uuij} = \left(\frac{b}{h}\right)^2 \mathscr{I}_{uiuj}^{1010} + \left(\frac{1-v}{2}\right)\left(\frac{a}{h}\right)^2 \mathscr{I}_{uiuj}^{0101} \tag{B4}$$

$$K_{uvij} = v\left(\frac{a}{h}\right)\left(\frac{b}{h}\right)\mathscr{I}_{uivj}^{1001} + \left(\frac{1-v}{2}\right)\left(\frac{a}{h}\right)\left(\frac{b}{h}\right)\mathscr{I}_{uivj}^{0110} \tag{B5}$$

$$K_{uwij} = \left(\frac{a}{h}\right)\left(\frac{b}{h}\right)\left(\frac{b}{R_x} + \frac{vb}{R_y}\right)\mathscr{I}_{uiwj}^{1000} \tag{B6}$$

$$K_{vvij} = \left(\frac{a}{h}\right)^2 \mathscr{I}_{vivj}^{0101} + \left(\frac{1-v}{2}\right)\left(\frac{b}{h}\right)^2 \mathscr{I}_{vivj}^{1010} \tag{B7}$$

$$K_{vwij} = \left(\frac{a}{h}\right)\left(\frac{b}{h}\right)\left(\frac{va}{R_x} + \frac{a}{R_y}\right)\mathscr{I}_{viwj}^{0100} \tag{B8}$$

$$K_{wwij} = \left(\frac{a}{h}\right)^2\left[\left(\frac{b}{R_x}\right)^2 + 2v\left(\frac{b}{R_x}\right)\left(\frac{b}{R_y}\right) + \left(\frac{b}{R_y}\right)^2\right]\mathscr{I}_{wiwj}^{0000}$$
$$+ \frac{1}{12}\left[\left(\frac{b}{a}\right)^2 \mathscr{I}_{wiwj}^{2020} + \left(\frac{a}{b}\right)^2 \mathscr{I}_{wiwj}^{0202} + v(\mathscr{I}_{wiwj}^{0220} + \mathscr{I}_{wiwj}^{2002}) + 2(1-v)\mathscr{I}_{wiwj}^{1111}\right] \tag{B9}$$

$$M_{uuij} = \mathscr{I}_{uiuj}^{0000} \tag{B10}$$

$$M_{vvij} = \mathscr{I}_{vivj}^{0000} \tag{B11}$$

$$M_{wwij} = \mathscr{I}_{wiwj}^{0000} \tag{B12}$$

and

$$\lambda = \omega ab\sqrt{\frac{\rho h}{D}}, \tag{B13}$$

where $i, j = 1, 2, \ldots, m$.